Available online at www.sciencedirect.com
ScienceDirect
Journal of Organometallic Chemistry 691 (2006) 4890–4900
Journal of Organometallic Chemistry
www.elsevier.com/locate/jorganchem

Synthesis and electrochemistry of late transition metal complexes containing 1,1′-bis(dicyclohexylphosphino)ferrocene (dcpf). The X-ray structure of [$PdCl_2$(dcpf)] and Buchwald–Hartwig catalysis using [$PdCl_2$(bisphosphinometallocene)] precursors

Laura E. Hagopian [a], Alison N. Campbell [a,1], James A. Golen [b,2], Arnold L. Rheingold [b], Chip Nataro [a,*]

[a] *Department of Chemistry, Lafayette College, Hugel Science Center, Easton, PA 18042, USA*
[b] *Department of Chemistry and Biochemistry, University of California, San Diego, La Jolla, CA 92093, USA*

Received 3 July 2006; received in revised form 14 August 2006; accepted 15 August 2006
Available online 22 August 2006

Abstract

The electrochemistry of 1,1′-bis(dicyclohexylylphosphino)ferrocene (dcpf) was examined in methylene chloride with tetrabutylammonium hexafluorophosphate or tetrabutylammonium tetrakis(pentafluorophenyl)borate as the supporting electrolyte. The oxidation of dcpf is complicated by a follow-up reaction. Seven new complexes containing dcpf and one new compound containing 1,1′-bis(di-*tert*-butylphosphino)ferrocene (dtbpf) were prepared and characterized. The new complexes were analyzed by cyclic voltammetry and the oxidation of these complexes occurred at a more positive potential than the free ligand. In addition, the X-ray structure of [$PdCl_2$(dcpf)] was determined and compared to other palladium complexes containing bisphosphinometallocene ligands. Five different palladium complexes containing bisphosphinometallocene ligands were examined as catalyst precursors in Buchwald–Hartwig catalysis.

Keywords: Electrochemistry; Cyclic voltammetry; Crystal structure; 1,1′-Bis(dicyclohexylphosphino)ferrocene; 1,1′-Bis(diphenylphosphino)ferrocene; Buchwald–Hartwig catalysis

1. Introduction

Palladium catalysts have become an important means of facilitating the formation of a variety of different bonds, including carbon–nitrogen [1–4], carbon–carbon [5–11], carbon–oxygen [12–14] and carbon–sulfur bonds [15,16]. Carbon–nitrogen bond formation via the Buchwald–Hartwig reaction, in which aryl amines (or aryl ethers) are formed using a palladium (0) catalyst containing chelating ligands, is of particular interest. The use of chelating ligands has been shown to improve the synthesis of arylamines by inhibiting competing reactions [3].

Bidentate phosphines, in particular those with a metallocene backbone, are one type of chelating ligands that have been investigated as ligands in Buchwald–Hartwig catalysis due to their unique steric and electronic properties. The most widely studied of these chelating phosphines is 1,1′-bis(diphenylphosphino)ferrocene (dppf) which has been shown to have numerous advantages as compared to 1,2-bis(diphenylphosphino)ethane (dppe) and 1,3-bis(diphenylphosphino)propane (dppp), which contain alkyl, rather than metallocene, backbones. For example, dppe and dppp

* Corresponding author. Fax: +1 610 330 5714.
E-mail address: nataroc@lafayette.edu (C. Nataro).
[1] Present address: Department of Chemistry, The University of North Carolina at Chapel Hill, Chapel Hill, NC 27599, USA.
[2] Permanent address: Department of Chemistry and Biochemistry, University of Massachusetts, Dartmouth, North Dartmouth, MA 02747, USA.

0022-328X/$ - see front matter © 2006 Elsevier B.V. All rights reserved.
doi:10.1016/j.jorganchem.2006.08.030

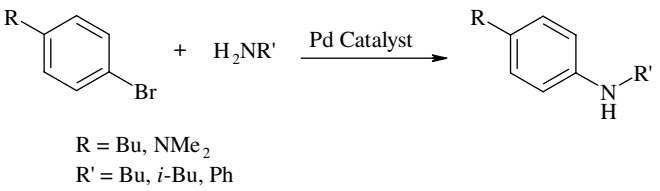

Scheme 1. Model reactions studied by Hamann and Hartwig.

undergo decomposition reactions and produce no arylamine products when used as ligands in a Buchwald–Hartwig coupling reaction [8]. However, using dppf as a ligand leads to intermediates which readily produce arylamines in the Buchwald–Hartwig reaction [17]. In fact, [$PdCl_2$(dppf)] has been reported to be one of the most efficient catalyst precursors for coupling primary amines and aryl halides [18]. Mechanistic studies of the Buchwald–Hartwig reaction have suggested that the steric nature, specifically the P–Pd–P bite angle, and electronic nature of the ligands play a role in the efficiency of the catalyst [2] (Scheme 1).

Although there have been several catalytic studies employing dppf, few have examined how changing the substituents on the phosphorus atoms of 1,1′-bis(phosphino)metallocene affects the catalytic activity. The study employing the largest variety of 1,1′-bis(phosphino)metallocene ligands focused on dppf derivatives in which there were different substituents added to the aromatic ring [2]. Numerous other 1,1′-bis(diorganophosphino)metallocene ligands and dichloropalladium complexes containing these ligands are known. The most commonly used derivatives of dppf are 1,1′-bis(diphenylphosphino)ruthenocene (dppr), 1,1′-bis(diisopropylphosphino)ferrocene (dippf), 1,1′-bis(dicyclohexylphosphino)ferrocene (dcpf) and 1,1′-bis(di-*tert*-butylphosphino)ferrocene (dtbpf). Palladium dichloride compounds of several 1,1′-bis(phosphino)metallocene ligands have been effectively used as catalyst precursors in a variety of catalytic systems such as the synthesis of oxindoles by amide α-arylation [19] and the arylation of ketones and malonates [20].

Of the previously mentioned 1,1′-bis(phosphino)metallocene ligands, dcpf and dtbpf have received the least attention. Most of the research focusing on dcpf involves Pd(II) derivatives used for catalysis [2–4]. The only study that directly compared dcpf and dppf containing catalyst precursors was for the alkoxycarbonylation of aryl chlorides and dcpf was found to be a better ligand [2]. Studies using dtbpf as a ligand have also been centered on palladium catalysts [4–15]. The bulkiness of dtbpf was proposed to be the key to its reactivity in catalytic applications [6,7,13–16]. For example, in the synthesis of oxindoles by amide α-arylation, the catalyst containing dtbpf was found to have similar catalytic abilities as the catalyst containing dcpf [4]. It was also determined that dtbpf was a better ligand than dppf in the reductive elimination of diaryl ethers [13], but it was a poorer ligand than dppf for hydrogenation reactions [16].

Examining a variety of palladium catalyst precursors containing 1,1′-bis(phosphino)metallocene ligands will result in a better understanding of how the sterics and electronics of these ligands affect catalytic efficiency. There is a limited understanding of how the steric and electronic properties of dcpf differ from those of other 1,1′-bis(diphosphino)metallocene ligands. To better understand the electronic nature of dcpf, the electrochemistry of dcpf and several new compounds containing dcpf was investigated. The X-ray structure of [$PdCl_2$(dcpf)] is presented and compared to analogous 1,1′-bis(phosphino)metallocene palladium dichloride complexes in order to examine the steric nature of dcpf. Finally, catalysis of the Buchwald–Hartwig reaction using five different [$PdCl_2$(P^P)] (P^P = dppf, dppr, dippf, dcpf and dtbpf) complexes as catalyst precursors, three different aryl bromides and four different amines was examined.

2. Experimental

2.1. General procedures

All reactions were completed under an argon atmosphere using Schlenk methods. Reagent-grade isopropanol, chloroform, ethanol, and methanol were used without additional purification. Tetrahydrofuran (THF) and diethyl ether (Et_2O) were distilled under a nitrogen atmosphere and refluxed over potassium benzophenone ketyl. Methylene chloride (CH_2Cl_2) and hexanes were distilled over CaH_2 under a nitrogen atmosphere. Electrochemistry was performed using HPLC grade CH_2Cl_2 that was distilled over CaH_2 under an argon atmosphere. NMR spectra were obtained on a JEOL Eclipse 400 FT-NMR in $CDCl_3$. TMS was used as an internal reference for ^1H NMR while 85% H_3PO_4 served as an external standard for $^{31}P\{^1H\}$ NMR. Analyses were carried out by Quantitative Technologies, Inc. UV–Vis experiments were conducted on a Beckman DU-65 spectrophotometer.

Ferrocene, decamethylferrocene, ruthenocene, chlorodicyclohexylphosphine, bis(benzonitrile)dichloropalladium, dppf, dippf and dtbpf were purchased from Strem. Ferrocene was sublimed prior to use. $NiCl_2 \cdot 6H_2O$, $PtCl_2(CH_3CN)_2$, $ZnCl_2$, $CdCl_2$, $HgCl_2$, tetrabutylammonium hexafluorophosphate ([NBu_4][PF_6]), cyclohexylamine, hexylamine, aniline, 2,6-dimethylaniline, bromobenzene, 4-bromotoluene, 4-bromotrifluorotoluene, potassium *tert*-butoxide, and decane were purchased from Aldrich. The [NBu_4][PF_6] was dried under vacuum with heating prior to use. The following compounds were prepared according to the literature procedures: dppr [21], dcpf [22], [$PdCl_2$(dppf)] [23], [$PdCl_2$(dppr)] [21], [$PdCl_2$(dippf)] [24], and [$PdCl_2$(dtbpf)] [25]. $HAuCl_4 \cdot H_2O$ was purchased from Fisher. $Li[B(C_6F_5)_4] \cdot (OEt_2)_{2.5}$ was obtained from Boulder Scientific and metathesized to ($[NBu_4]^+$ $[B(C_6F_5)_4]^-$) in accordance with the literature [26].

2.2. Synthesis

2.2.1. [$NiCl_2$dcpf)] (**1**)

A solution of dcpf (0.0984 g, 0.170 mmol) in 30 mL of isopropanol was heated in a warm water bath (~85 °C). A solution of $NiCl_2 \cdot 6H_2O$ (0.0404 g, 0.170 mmol) in 15 mL of isopropanol/methanol (2:1 v/v) was stirred for 15 min and transferred by filter cannula into the dcpf solution. The resulting mixture was refluxed for 3 h and then filtered. The precipitate was washed with 10 mL of Et_2O, then 10 mL of CH_2Cl_2, yielding a gray-green solid. A second crop of product was obtained by cooling the initial filtrate in the freezer. These crystals were added to the first crop of product to give a total of 0.0609 g (51%) of **1**. Anal. Calc. for $C_{34}H_{52}Cl_2FeNiP_2 \cdot 1/4\,CH_2Cl_2$: C, 56.40; H, 7.26. Found: 56.78, 7.33%. UV–Vis (CH_2Cl_2, λ nm, ε L/(cm mol)): 607 (264).

2.2.2. [$PdCl_2$(dcpf)] (**2**)

$PdCl_2(C_6H_5CN)_2$ (0.1335 g, 0.3481 mmol) and dcpf (0.1992 g, 0.3443 mmol) were dissolved in 10 mL of CH_2Cl_2 and stirred for 2 h. The solution was initially dark brown but, after stirring, turned a lighter brown, and a precipitate appeared. Et_2O (20 mL) was added and the reaction mixture was stirred for 5 min. The solution was subsequently filtered, and the resulting liquid was concentrated, layered with Et_2O, and cooled in the freezer, yielding red crystals of **2** (0.1424 g, 55%). Anal. Calc. for $C_{34}H_{52}Cl_2FeP_2Pd$: C, 54.02; H, 6.93. Found: 54.05, 6.93%. $^{31}P\{^1H\}$ ($CDCl_3$): δ 56.6 (s). ^1H NMR ($CDCl_3$): δ 4.54 (s, 4H, C_5H_4), 4.46 (s, 4H, C_5H_4), 2.7–1.0 (m, 44H, Cy).

2.2.3. [$PtCl_2$(dcpf)] (**3**)

$PtCl_2(CH_3CN)_2$(0.0206 g, 0.0588 mmol) and dcpf (0.0347 g, 0.0600 mmol) were dissolved in 3 mL of CH_2Cl_2 and stirred for 1 h. The resulting solution was concentrated to one third its original volume, layered with Et_2O, and cooled in the freezer for three days to form crystals. The solution was subsequently filtered, and the crystals were washed with 5 mL Et_2O, giving **3** as a yellow solid (0.0147 g, 30%). Anal. Calc. for $C_{34}H_{52}Cl_2FeP_2Pt \cdot Et_2O$: C, 49.68; H, 6.80. Found: 50.08, 6.56%. $^{31}P\{^1H\}$ ($CDCl_3$): δ 23.0 (s, $^1J_{P-Pt} =$ 3800 Hz). ^1H NMR ($CDCl_3$): δ 4.44 (s, 4H, C_5H_4), 4.43 (s, 4H, C_5H_4), 2.7–1.0 (m, 44H, Cy).

2.2.4. [Au_2Cl_2(dcpf)] (**4**)

$HAuCl_4 \cdot H_2O$ (0.224 g, 0.626 mmol) was dissolved in a mixture of 1.5 mL of water and 8.0 mL of methanol, and the solution was cooled to 0 °C. A solution of $S(CH_2CH_2OH)_2$ (0.8 mL, 8 mmol) in 1.5 mL of methanol was added, and the resulting mixture was stirred for 15 min. dcpf (0.2610 g, 0.4511 mmol) was dissolved in a minimal amount of chloroform and then added to the mixture. The reaction was allowed to stir for 6 h while slowly warming to room temperature. Methanol (25 mL) was added, and the resulting solution was concentrated to approximately 12 mL. Et_2O (20 mL) was then added, and the solution was filtered to give a solid. This solid was washed with methanol to yield **4** as a yellow solid (0.0594 g, 18%). Anal. Calc. for $C_{34}H_{52}Cl_2FeP_2Au_2$: C, 39.14; H, 5.02. Found: 39.40, 5.24%. $^{31}P\{^1H\}$ ($CDCl_3$): δ 41.2 (s). ^1H NMR ($CDCl_3$): δ 4.72 (s, 4H, C_5H_4), 4.43 (s, 4H, C_5H_4), 2.7–0.9 (m, 44H, Cy).

2.2.5. [$ZnCl_2$(dcpf)] (**5**)

A solution of dcpf (0.0668 g, 0.115 mmol) in 12 mL of isopropanol was heated in a warm water bath (~85 °C). A solution of $ZnCl_2$ (0.0161 g, 0.118 mmol) in 2.3 mL of an isopropanol/methanol mixture (2:1 v/v) was added. The resulting solution was refluxed for 2 h and cooled overnight in the freezer. The solution was filtered, and the resulting solid was washed with Et_2O and dried to isolate **5** as a pale orange solid (0.0321 g, 39%). Anal. Calc. for $C_{34}H_{52}Cl_2FeP_2Zn$: C, 57.13; H, 7.31. Found: 56.87, 7.38%. $^{31}P\{^1H\}$ ($CDCl_3$): δ −15.15 (s). ^1H NMR ($CDCl_3$): δ 4.46 (br s, 8H, C_5H_4), 2.3–1.2 (m, 44H, Cy).

2.2.6. [$CdCl_2$(dcpf)] (**6**)

A solution of dcpf (0.0578 g, 0.0999 mmol) in 4 mL of isopropanol was heated in a warm water bath (~85 °C). A solution of $CdCl_2$ (0.0183 g, 0.0998 mmol) in 6 mL of an isopropanol/methanol mixture (2:1 v/v) was added to the dcpf solution. The resulting solution was refluxed for 2 h, filtered, and the resulting solid was washed with Et_2O, yielding **6** as a pale orange solid (0.0377 g, 50%). Anal. Calc. for $C_{34}H_{52}Cl_2FeP_2Cd$: C, 53.60; H, 6.88. Found: 53.33, 6.88%. $^{31}P\{^1H\}$ ($CDCl_3$): δ 2.48 (s, $^1J_{P-Cd} = 1450$ Hz, $^1J_{P-Cd} =$ 1380 Hz). ^1H NMR ($CDCl_3$): δ 4.53 (s, 4H, C_5H_4), 4.34 (s, 4H, C_5H_4), 2.3–1.2 (m, 44H, Cy).

2.2.7. Mercury compounds

*2.2.7.1. [$HgCl_2$(dcpf)] (**7a**).* $HgCl_2$ (0.0478 g, 0.176 mmol) and dcpf (0.1018 g, 0.176 mmol) were added to 150 mL of refluxing ethanol and refluxed for an additional 5 min. Upon cooling to room temperature, the solution was concentrated to approximately 30 mL and filtered to give a yellow solid. The solid was recrystallized by dissolving in CH_2Cl_2, layering with Et_2O, and cooling in the freezer. The crystals were collected by filtration and washed with Et_2O. The combined filtrates were dried *in vacuo* and the resulting solid was recrystallized from a mixture of CH_2Cl_2 and Et_2O to give a second crop of crystals which was isolated by filtration. This second batch of crystals was washed twice with Et_2O and combined with the first batch to give **7a** as a dark yellow solid (0.0857 g, 57%). Anal. Calc. for $C_{34}H_{52}Cl_2FeP_2Hg$: C, 48.04; H, 6.17. Found: 47.89, 6.31%. $^{31}P\{^1H\}$ ($CDCl_3$): δ 30.98 (s, $^1J_{P-Hg} =$ 4130 Hz). ^1H NMR ($CDCl_3$): δ 4.56 (s, 4H, C_5H_4), 4.41 (s, 4H, C_5H_4), 2.5–1.2 (m, 44H, Cy).

*2.2.7.2. [$HgCl_2$(dtbpf)] (**7b**).* Prepared by a method analogous to the preparation of **7a**, **7b** was isolated as an orange solid (0.0864 g, 66%). Anal. Calc. for $C_{26}H_{44}Cl_2FeP_2Hg$: C, 41.86; H, 5.95. Found: 41.78, 5.94%. $^{31}P\{^1H\}$ ($CDCl_3$): δ 61.42 (s, $^1J_{P-Hg} = 4260$ Hz). ^1H NMR ($CDCl_3$): δ 4.63 (s, 4H, C_5H_4), 4.59 (s, 4H, C_5H_4), 1.63 (dd, 36H, CH_3).

2.3. X-ray crystallography

Crystals of **2a** · $2CH_2Cl_2$ were formed by the diffusion of Et_2O into a solution of **2** in CH_2Cl_2. A yellow-orange colored crystal, approximately $0.20 \times 0.20 \times 0.05$ mm^3 in size, was mounted on a glass fiber with epoxy and cooled to −55 °C. Diffraction intensity data were collected with a Siemens/Bruker Smart Apex CCD diffractometer using Mo Kα radiation at −55 °C. Additional crystal, data collection, and refinement parameters are given in Table 1. The structure was solved using direct methods, completed by subsequent difference Fourier syntheses, and refined by full matrix least-squares procedures on F^2. Sources of software and scattering factors are contained in the SHELXTL (5.10) program package (G. M. Sheldrick, Bruker AXS, Madison, WI) [27]. SADABS absorption corrections were applied to all data. All non-hydrogen atoms (except C13, C14 and C16) were refined with anisotropic displacement coefficients and hydrogen atoms were treated as idealized contributions. Three of the C atoms (C13, C14, and C16) of one cyclohexyl ring were disordered over two positions at 51.67% occupancy. No hydrogen atoms were placed on this ring. One of the CH_2Cl_2 solvent molecules was disordered and on a center of symmetry. It was treated by using the Platon Program Squeeze (found for the unit cell 113.3 e/Å^3, calculated 96 e/Å^3 and 118 e/Å^3 if the missing H atoms included) [28]. There were two residual peaks greater than 1 e/Å^3, Q1 1.06 e/Å^3 and Q2 1.03 e/Å^3 were found respectively at 0.837 and 0.872 Å of Pd1.

Table 1
Crystal data and structure analysis results of **2**

	$PdCl_2$(dcpf) · 2 CH_2Cl_2
Empirical formula	$C_{36}H_{56}Cl_6FeP_2Pd$
Formula weight	925.70
Crystal system	Triclinic
Space group	$P\bar{1}$
a (Å)	9.8245(5)
b (Å)	9.8374(5)
c Å	20.4247(11)
α (°)	97.8070(10)
β (°)	97.8700(10)
γ (°)	90.8210(10)
V (Å^3)	1936.19(17)
Z	2
Crystal size (mm)	$0.20 \times 0.20 \times 0.05$
Crystal color	Yellow-orange
radiation; λ (Å)	0.71073
Temperature, K	218(2)
θ Range (°)	2.03–28.33
Data collected	
h	−12 to 11
k	−13 to 13
l	−26 to 23
No. of data collected	13,916
No. of unique data	8693
Absorption correction	Multiscan/SADABS
Final R indices (observed data)	
R_1	0.0475
wR_2	0.1189
Goodness of fit	1.040

2.4. Electrochemistry

The oxidative electrochemistry of all compounds was examined in CH_2Cl_2 under an argon atmosphere at ambient temperature (22 ± 1 °C). The supporting electrolyte was 0.1 M [NBu_4][PF_6] and the concentration of the analyte was 1.0 mM. Additional electrochemical studies of dcpf were carried out in 0.50 M [NBu_4][$B(C_6F_5)_4$], with analyte concentrations of 0.50 mM, 1.0 mM, and 2.0 mM. Data were collected at −10, 0, 10, and 20 ± 0.1 °C and scan rates ranging between 25 and 500 mV/s. For all experiments, the counter electrode was a platinum wire, and the reference electrode was non-aqueous silver/silver chloride separated from the solution by a fine glass frit. The working electrode was 1.5 mm diameter glassy carbon which was polished with 1 μm diamond paste, rinsed with acetone, polished with 0.25 μm diamond paste, and rinsed with CH_2Cl_2 prior to use. The potentials were indirectly referenced to ferrocene by the addition of decamethylferrocene at the end of the experiment [29]. The cyclic voltammagrams were obtained using a Princeton Applied Research 263-A potentiostat, and the resulting data were collected and analyzed with Power Suite. All simulations were carried out by DIGISIM (Bioanalytical Systems) [30].

2.5. Catalytic studies

2.5.1. Amination of aryl halides

In a typical reaction, 5 mol% of the catalyst, 15 mol% of the corresponding free ligand and potassium *tert*-butoxide (19.2 mg, 0.171 mmol) were placed in a screw-cap NMR tube. The NMR tube was brought into a glovebox where degassed THF (0.50 mL) and aryl bromide (0.137 mmol) were added. The tube was sealed with a cap containing a PTFE septum and was removed from the glovebox. The appropriate amine (0.171 mmol) was added via syringe through the septum and the reaction mixture was heated to 100 °C for 3 h. The reaction was then allowed to cool to room temperature. THF was added to the reaction mixture, bringing the total volume to 1.5 mL and the resulting solution was mixed thoroughly. After precipitate settled, two 0.5 mL aliquots of the mixture were transferred to screw-cap vials with TFE septa. Decane (2.0 μL) was added to each duplicate as an internal standard. The samples were then analyzed by GC/MS. All GC/MS analyses were carried out on a Fisons Instruments 8030 gas chromatograph equipped with a Fisons MD800 mass spectral analyzer. The gas-chromatograph employed an Alltech ECONOCAP Faster Fatty Acid Phase column, with phase SE-54, and dimensions 30 m × 0.25 mm ID × 0.25 μm. Lab-Base 2 data system for DOS was used for data analysis. The area of each peak was computer integrated. A ratio of peak area to concentration of analyte was established for both the decane and the reaction product, and this was used to determine the product yield for each reaction.

2.5.2. Isolation of arylamine product

The product of the reaction of aniline with bromotoluene was isolated and purified in order to confirm its identity. The reaction of aniline with bromotoluene was carried out as described above with [$PdCl_2$(dppf)] used as the catalyst precursor. The reaction was allowed to cool to room temperature and the solvent was removed. The remaining oil was dissolved in minimal diethyl ether and applied to a short silica column. The column was washed with a mixture of hexanes and diethyl ether (10:1) and the purified desired product was eluted with a 5:1 mixture of hexanes and diethyl ether. The identity of the product was confirmed by ^{1}H NMR and GC/MS.

3. Results and discussion

Electrochemical studies of dcpf were carried out at a variety of temperatures and concentrations. The cyclic voltammagrams of dcpf were analyzed and the potential at which oxidation occurs (E^0) is 0.02 V relative to $FcH^{0/+}$. This is similar to the potentials at which oxidation of the closely related dippf (0.05 V vs. $FcH^{0/+}$) [31] and dtbpf (0.06 V vs. $FcH^{0/+}$) [32] occur and is significantly less positive than the potential at which oxidation of dppf occurs [23]. The electrochemical parameter, E_L, is defined as $1/2E^0$ (Fe^{III}/Fe^{II}) (vs. NHE) for symmetric ferrocenes; E_L was determined to be 0.34 V for dcpf [33]. The E_L value can be used to estimate the Hammett parameter for derivatives of ferrocene with the equation $E_L = 0.45\sigma_p + 0.36$. Using this data, the σ_p value for the –PCy_2 group can be estimated as −0.04.

The reversibility of the dcpf wave was found to be largely dependent on temperature, scan rate, and concentration (Fig. 1). The chemical reversibility parameter (i_r/i_f) for dcpf was calculated at a variety of temperatures and concentrations (Table 2) [34,35]. At slow scan rates, the oxidized form of dcpf appears to undergo a reaction which is proposed to be an EC dimerization [36] similar to that of dppf [37] and dippf [31] (Scheme 2). Using the chemical reversibility parameter, the second order rate constant of an EC dimerization reaction (k_d) was calculated at various temperatures [35].

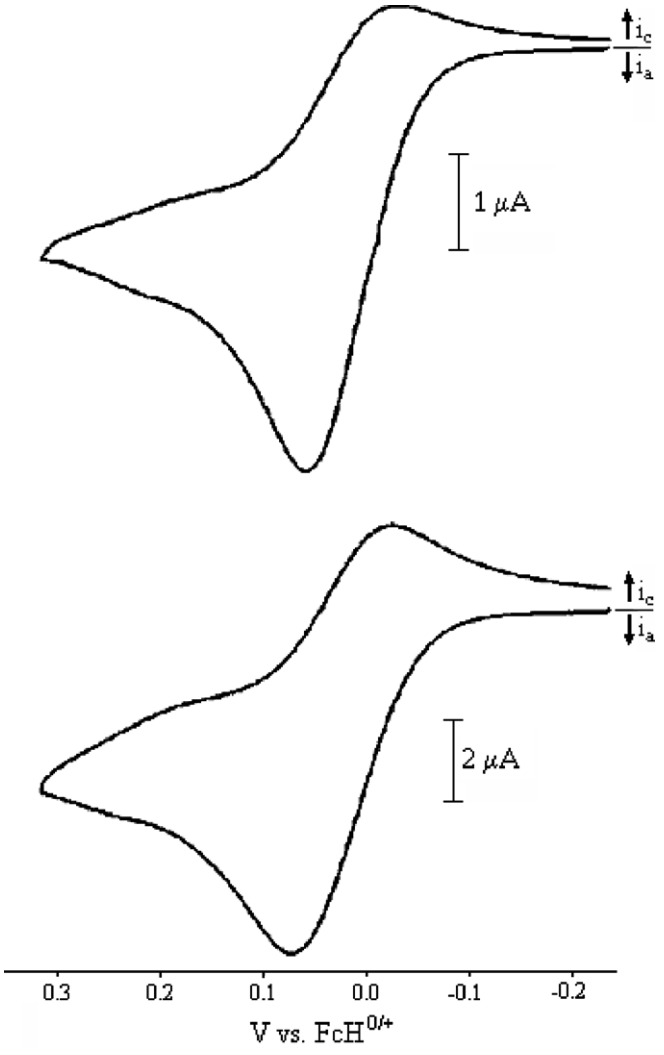

Fig. 1. Cyclic voltammagrams of 1.0 mM dcpf in CH_2Cl_2 with 0.05 M [NBu_4][$B(C_6F_5)_4$] supporting electrolyte. Scans were run at 293 K at scan rates of 25 mV/s (top) and 100 mV/s (bottom).

Table 2
Reversibility and second-order rate constants for the oxidation of dcpf

	−10 °C	0 °C	10 °C	20 °C
Reversibility (i_r/i_f)				
0.50 mM	0.58	0.54	0.53	0.51
1.0 mM	0.56	0.51	0.49	0.45
2.0 mM	0.55	0.50	0.47	0.43
Rate constant [10^2 k_d (M^{-1} s^{-1})]				
Experimental	2.0	3.6	4.9	6.6
Simulated	4.3	6.6	10	14

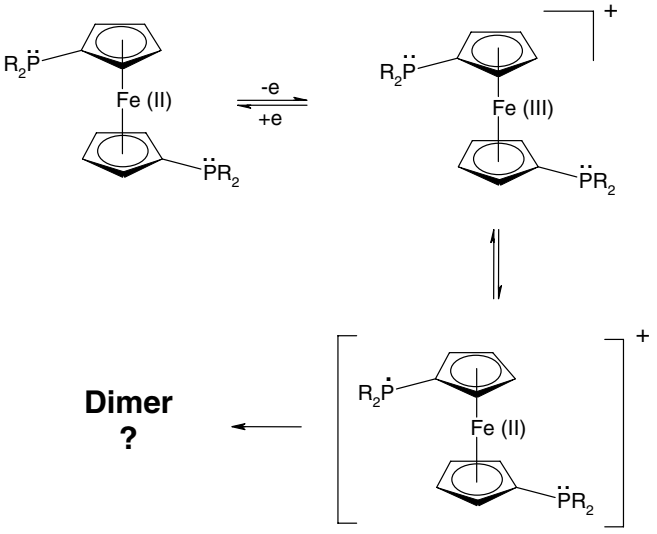

Scheme 2. Proposed dimerization reaction of 1,1′-bis(diphosphino)-ferrocenes.

The dimerization reaction was also simulated using DIGISIM, and theoretical cyclic voltammagrams were compared to the experimental data (Fig. 2). An Arrhenius relationship (Fig. 3) was used to determine the activation parameters from the rate constants. The experimental values for $\Delta H^{\ddagger}$ and $\Delta S^{\ddagger}$ were 22 ± 1 kJ/mol and -220 ± 10 J/K mol, respectively, while the simulated values for $\Delta H^{\ddagger}$ and $\Delta S^{\ddagger}$ were 23 ± 1 kJ/mol and -220 ± 10 J/K mol. When compared to dppf and dippf, the experimental and theoretical $\Delta S^{\ddagger}$ values for the EC dimerization are identical. However, the enthalpies of dimerization are not equivalent; dcpf has a lower $\Delta H^{\ddagger}$ than dppf and a higher $\Delta H^{\ddagger}$ than dippf [31,37]. The difference between the $\Delta H^{\ddagger}$ of dimerization for dppf and dcpf can be attributed to the phenyl groups of dppf which can participate in delocalization of the proposed phosphorus radical, making the cation less likely to dimerize. The difference in the $\Delta H^{\ddagger}$ of dimerization for dippf and dcpf is likely due to the difference in the steric bulk of the groups; the cone angle of PCy_3 is 170° while that of $P(i\text{-}Pr)_3$ is 160° [38].

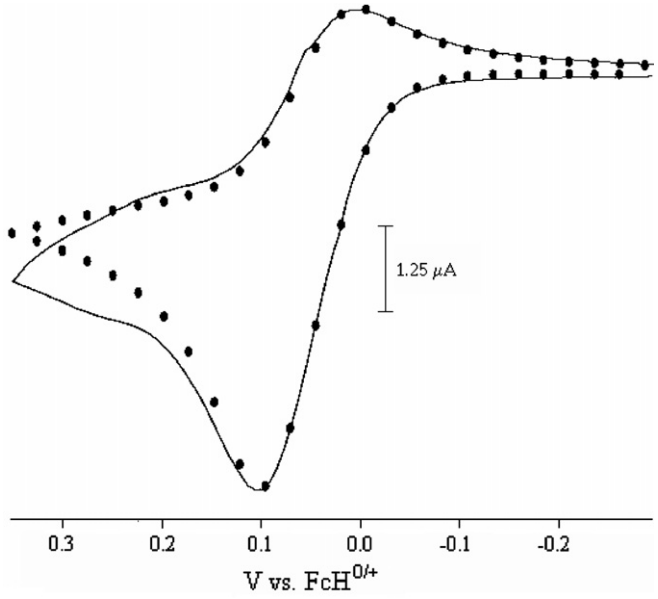

Fig. 2. Experimental (–) and simulated (●) cyclic voltammagrams for 1.0 mM dcpf in methylene chloride at 273 K with a scan rate of 100 mV/s.

A total of eight new compounds containing either dcpf or dtbpf were synthesized and characterized. In most cases, both the dcpf and dtbpf [32] compounds have been prepared, however, after repeated attempts, the Zn, and Cd derivatives of dtbpf could not be isolated. This is likely due to steric effects; the bulkier *tert*-butyl groups of dtbpf prevent coordination of dtbpf to the relatively small Zn or Cd centers. In addition, it is likely that the bulk of the dtbpf ligand plays a role in the synthetic procedures; it was necessary to stir and/or reflux the reactions for preparing the dtbpf complexes for twice as long as their dcpf analogues.

Of all the compounds synthesized, only compound **1** was paramagnetic. The magnetic moment, μ_B, was determined to be 3.0 by the Evans Method [39]. This value is similar to the values for the corresponding dppf [37] and dippf [31] compounds and is in the range expected for Ni(II) complexes in pseudo-tetrahedreal geometries [40]. To further characterize **1**, the visible spectrum was obtained. A 0.0010 M solution of **1** in CH_2Cl_2 was scanned between 400 and 800 nm, and a peak was found at 607 nm. The λ_{max} and extinction coefficient are similar to those seen in the spectra of the dppf [37] and dippf [31] analogues.

The remaining compounds, **2**–**7**, were diamagnetic and could easily be characterized by $^{31}P\{^1H\}$ and ^1H NMR. With the exception of the zinc compound, the coordination of the bidentate phosphine to a metal center resulted in a downfield shift in the $^{31}P\{^1H\}$ NMR. In addition, for the Zn, Cd, and Hg dcpf compounds, the $^{31}P\{^1H\}$ signal shifted downfield going down the group. Also noteworthy are the coupling constants observed in the $^{31}P\{^1H\}$ NMR for **3**, **6**, and **7** which clearly show that the ligand is coordinated to metals with NMR active isotopes. In general, the spectral data for **2**–**7** are similar to those reported for the dippf analogues [31].

A crystal of **2** was obtained, and its structure was determined by X-ray crystallography (Fig. 4). Selected bond angles and lengths are given in Table 3. This is the first X-ray structure of a compound containing dcpf to

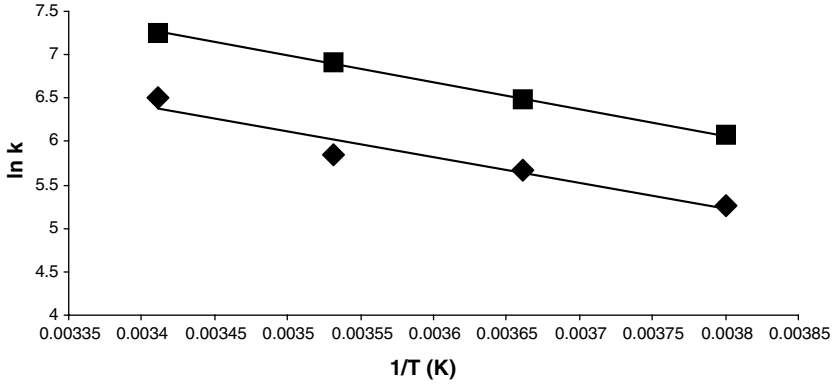

Fig. 3. Arrhenius plot of experimental (◆) and simulated (■) rate data for dcpf. For the experimental data, the slope was −2984, the intercept was 16.6, and R^2 was 0.9369. For the simulated data, the slope was −3068, the intercept was 17.7, and R^2 was 0.9995.

be determined. The dcpf ligand adopts a synclinal staggered arrangement about the Pd atom; this is the most common arrangement for coordinated dppf [41]. Pd adopts a pseudo-square planar geometry with the two P atoms cis, similar to dppf and dippf analogues [24,25]. In addition, the P–Pd–P angle of 102.45° is 4.47° larger than the corresponding angle of the dppf analogue [25] and 2.43° larger than the corresponding angle of the dppr analogue [37] (Table 4); this difference can be attributed to the steric hindrance of the bulky cyclohexyl groups [42]. However, it is somewhat surprising that the corresponding angle in the dippf analogue is 1.14° larger than the angle in **2** [31]. PCy_3 has a larger cone angle than $P(i\text{-}Pr)_3$ [38], so it was anticipated that the P–Pd–P angle would be larger for $PdCl_2$(dcpf) (**2**). The difference may be attributed to packing of the molecules in the crystal.

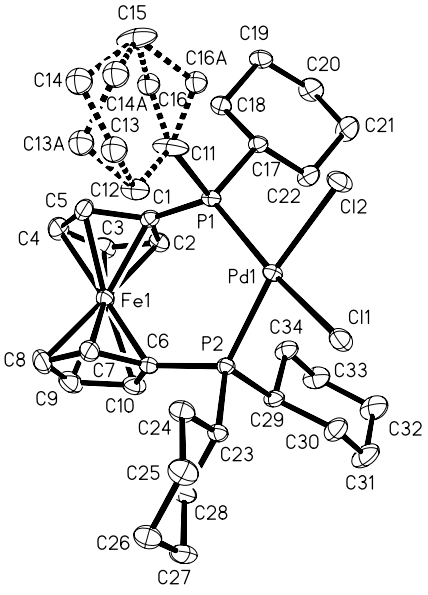

Fig. 4. ORTEP diagram of [$PdCl_2$(dcpf)].

Table 3
Selected bond lengths (Å) and angles (°) for compound **2**

Bond lengths			
Average P–Pd	2.287	Average Pd–Cl	2.353
Average Fe–C	2.035	P–P	3.566
Average δ_p[a]	−0.114		
Bond angles			
P–Pd–P	102.45(3)	Cl–Pd–Cl	87.49(3)
P(1)–Pd–Cl(1)	169.11(3)	P(1)–Pd–Cl(2)	84.53(3)
P(2)–Pd–Cl(1)	86.36(3)	P(2)–Pd–Cl(2)	170.51(4)
X_a–Fe–X_b[b]	178.32	P–Fe–P	61.88
τ[c]	21.27	θ[d]	2.25

[a] Deviation of the P atom from the Cp plane; the negative value here means that the P is farther from the Fe.
[b] Centroid–Fe–centroid.
[c] Torsion angle C_A–X_A–X_B–C_B where C is the carbon bonded to P and X is the centroid.
[d] The dihedral angle between the two Cp rings.

Table 4
P–Pd–P bite angle for various [$PdCl_2$(bisphosphinometallocene)] complexes

Compound	Bite angle	Reference
[$PdCl_2$(dppf)]	97.98(4)	[25]
[$PdCl_2$(dppr)]	100.02(17)	[37]
[$PdCl_2$(dppo)][a]	100.82(9)	[47]
[$PdCl_2$(dcpf)]	102.45(3)	This work
[$PdCl_2$(dippf)]	103.59(4)	[24]
[$PdCl_2$(dmpf)][b]	99.30[c]	[48]

[a] dppo = 1,1′-bis(diphenylphosphino)osmocene.
[b] dmpf = 1,1′-bis(dimethylphosphino)ferrocene.
[c] Average of two crystallographically independent molecules.

The oxidative electrochemistry of compounds **1**–**7** was also investigated, and, upon coordination, oxidation of the iron center shifts to more positive potentials (Table 5). A similar trend has been noted for compounds containing dppf, dippf and dtbpf ligands [31,32,37]. The data show that potentials at which oxidation of derivatives of dcpf and dtbpf are similar to their dippf analogues but less positive than the dppf analogues [31,32,37]. This difference can be attributed to the more donating nature of alkyl groups as compared to aryl groups [43]. In addition, the data demonstrate that when dcpf binds to a 3d metal, the oxidation occurs at a less positive potential than when it binds to a 4d or 5d metal. Although a similar trend is observed for dippf, an explanation for this observation is not apparent at this time [31].

In addition, the oxidation for most of the complexes containing dcpf was chemically and electrochemically reversible. For dcpf, coordination to a metal center occupies the lone pair on the phosphorus atom and therefore prevents dimerization. The oxidation of compounds **1**, **5**, and **6** was on chemically reversible at higher scan rates, as were the oxidations of the dppf, dippf and dtbpf analogues of **1** and the dppf and dippf analogues of **6** [31,32,37]. It has been proposed that the bidentate phosphines bind weakly to the metal centers in these compounds and form highly reactive cations upon oxidation

Table 5
Oxidation potentials and chemical reversibility parameters (at 100 mV/s scan rate) for dcpf, dtbpf, and compounds **1**–**7**

Compound	E^0 (V) vs. $FcH^{0/+}$	i_p^{ox}/i_p^{red}
dcpf	0.02[a]	0.45
1	0.30[b]	0.84
2	0.47	0.95
3	0.46	0.94
4	0.52	0.95
5	0.33[b]	0.89
6	0.42[b]	0.80
7a	0.46[c], 0.62[b]	0.42, 0.89
dtbpf [28]	0.06[a]	0.98
7b	0.43[c], 0.57[b]	0.00, 0.83

[a] At 20 °C.
[b] Chemically and electrochemically reversible at higher scan rates.
[c] Chemically irreversible.

[23,31]. While the oxidation of **5** was chemically reversible at higher scan rates, the oxidation of its dppf and dippf analogues was chemically irreversible [23,31]. This incongruity can be attributed to the greater electron-donating ability of cyclohexyl groups as compared to phenyl and isopropyl groups [43]. It is possible that the more σ-donating cyclohexyl groups make the phosphorus atoms more electron rich, which leads to stronger metal–phosphorus bonds. These stronger bonds are less likely to break and lead to side products. Finally, compounds **7a** and**7b** were unique because they had more than one wave. Compound **7a** produced two distinct, chemically reversible waves at higher scan rates due to the oxidation of both mercury and iron. The dppf analogue of **7** displayed two chemically irreversible waves, suggesting that the σP → M bond of the dppf derivative breaks more easily and leads to the formation of side products [23]. However, the proposed stronger P–M bond in compound **7a** prevents side product formation. Oxidation of **7b** produced three waves at scan rates below 100 mV/s. At higher scan rates, there were only two waves which suggests that the third wave observed at low scan rates likely resulted from a side reaction. Of the two waves observed at higher scan rates, one was chemically reversible at high scan rates and the other was chemically and electrochemically reversible.

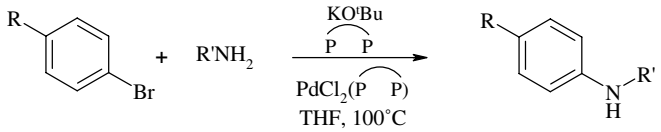

R = H, Me, CF_3

R' = cyclohexyl, hexyl, phenyl

P P = dppf, dppr, dippf, dcpf, dtbpf

Scheme 3. General reaction schemes for catalytic reactions.

With the electrochemical and structural data in hand, the complexes $[PdCl_2(P \cdot P)]$ ($P \cdot P$ = dppf, dppr, dippf, dcpf and dtbpf) were used as catalyst precursors in the Buchwald–Hartwig coupling reaction. The general reaction for the studied system is shown in Scheme 3 and the conditions employed were similar to a previous study [18]. All five of the palladium dichloride catalysts led to the formation of the arylamine product for each aryl bromide and primary amine combination. The GC yields for each combination of catalyst, amine, and aryl bromide were calculated and are reported in Table 6. The yields were comparable to those previously described for the amination of aryl bromides by palladium catalysts containing bidentate phosphine ligands [2]. Each catalyst contained a bidentate phosphine with a unique combination of steric and electronic properties which affected the rate of the reaction. The catalytic mechanism for arylamine formation can help to explain the differences in product yield based on varying sterics and electronics.

A recent reexamination of the mechanism for the catalytic coupling of aryl bromides and primary amines has been carried out by Buchwald and Hartwig [1]. In this reexamination, a palladium (0) species, $Pd(BINAP)_2$, was determined to be present in the solution but not an active part of the catalytic cycle [1]. A $^{31}P\{^1H\}$ NMR of the $[PdCl_2(dppf)]$ catalyzed coupling of 4-bromotoluene to cyclohexylamine displayed a major resonance at 25.1 ppm (THF-d_8). The $^{31}P\{^1H\}$ NMR shift of $Pd(dppf)_2$ was reported to be 24.1 ppm (in C_6D_6) [44] indicating that $Pd(dppf)_2$ is present in the reaction mixture. In the proposed mechanism, the active state of the catalyst, Pd(dppf), is in equilibrium with the inactive $Pd(dppf)_2$ [1]. The first step in the catalytic cycle involves the oxidative addition of the aryl bromide to Pd(dppf) followed by substitution of the bromide by the deprotonated amine. This generates an amido aryl palladium (II) intermediate. The formation

Table 6
GC yields (%) for all catalytic reactions run in THF at 100 °C for 3 h

Bromide	Catalyst precursor	Primary amine			
		Cyclohexylamine	Hexylamine	Aniline	2,6-Dimethylaniline
Bromotoluene	$PdCl_2$(dppf)	60	70	33	14
	$PdCl_2$(dppr)	35	35	57	37
	$PdCl_2$(dippf)	39	31	49	30
	$PdCl_2$(dcpf)	11	21	18	21
	$PdCl_2$(dtbpf)	39	27	21	15
Bromobenzene	$PdCl_2$(dppf)	67	36	18	18
	$PdCl_2$(dppr)	25	18	34	34
	$PdCl_2$(dippf)	39	50	34	40
	$PdCl_2$(dcpf)	2	34	24	<1
	$PdCl_2$(dtbpf)	14	39	3	7
Bromotrifluorotoluene	$PdCl_2$(dppf)	21	22	4	2
	$PdCl_2$(dppr)	37	23	9	5
	$PdCl_2$(dippf)	4	24	9	5
	$PdCl_2$(dcpf)	13	27	8	<1
	$PdCl_2$(dtbpf)	2	27	22	1

of the product is the result of reductive elimination of arylamine from the amido aryl palladium (II) intermediate.

Several other processes that compete with reductive elimination and lead to undesired byproducts have been reported [2]. The formation of arene and imine products due to β-H elimination has frequently been observed in systems using monodentate phosphine ligands [4]. However, it has also been demonstrated, based on mechanistic data, that the use of bidentate phosphine ligands inhibits β-H elimination, thus inhibiting the formation of undesired arene byproduct [17]. The presence of arene was very infrequent in the reactions carried out in this study, likely due to the inhibition of β-H elimination by the bidentate phosphines. Another byproduct reported in the literature was diarylamine [2]. However, this was not observed in any of the reactions carried out in this study. The main byproduct observed in this study was the coupling of the aryl groups of the aryl bromide to form the biphenyl analogue of the starting material.

Because the catalytic mechanism involves both oxidative and reductive processes, the electronic properties of the catalyst are expected to play a critical role in determining the efficiency of the catalyst and rate of catalysis. An electron-rich catalyst will favor the oxidative addition step in the catalytic mechanism while an electron-poor catalyst will favor the reductive elimination step. In order to explore the electronic properties of the catalysts, oxidative electrochemistry data and titration calorimetry data were examined. Based on the electrochemistry, the alkyl groups of dippf, dcpf, and dtbpf make the catalysts containing these ligands more electron-rich than the catalysts containing dppf and dppr [31,32,37]. Additionally, based on heat of protonation values, dppr has been previously determined to be slightly more basic than dppf [45].

In addition to electronics, steric effects were also expected to influence the catalytic system. Each catalyst has a unique bite angle (P–Pd–P) that affects the addition of substrate and elimination of product. A large bite angle may make oxidative addition more difficult because the substrate being added will have less room to fit onto the palladium center. However, a large bite angle may encourage reductive elimination to relieve steric strain on the catalyst. The sterics of the catalysts were compared by examining P–Pd–P bite angles from X-ray crystallographic data which has been reported for all of the palladium catalysts except [$PdCl_2$(dtbpf)]. [$PdCl_2$(dppf)] has the smallest bite angle [5], [$PdCl_2$(dippf)] [31] and [$PdCl_2$(dcpf)] have larger bite angles and [$PdCl_2$(dppr)] [37] falls in between. Although the bite angle of [$PdCl_2$(dtbpf)] has not been determined, it is anticipated to be similar to or slightly larger than the bite angles of [$PdCl_2$(dippf)] and [$PdCl_2$(dcpf)]. Therefore, [$PdCl_2$(dippf)], [$PdCl_2$(dcpf)] and [$PdCl_2$(dtbpf)] are the more electron rich catalyst precursors and are also the catalyst precursors with the largest bite angles. [$PdCl_2$(dppf)] and [$PdCl_2$(dppr)] are less electron rich than the complexes with ligands containing alkyl groups and have smaller bite angles than the analogous alkyl substituted complexes.

In addition to altering the catalysts, substrates with different electronic and steric properties should also influence the catalytic process. Substrates were chosen to selectively vary the steric environment and electronics of the system and to probe the effects of these changes on the catalytic efficiency. To study electronic effects, three aryl bromides with different substituents in the four-position were selected. Based on the Hammet parameters, the groups in the four-position were electronically neutral (*H*, 0.0), electron donating (CH_3, −0.17) and electron withdrawing (CF_3, 0.54) [46]. The use of four different primary amines also contributed to both the electronic and steric perturbations of the system. Electronically, cyclohexylamine and hexylamine are similar. However, the bulky cyclohexyl ring of cyclohexylamine makes it more sterically hindered. Compared to both cyclohexylamine and hexylamine, aniline and 2,6-dimethylaniline are both less electron rich. In addition, the methyl groups in the two and six positions of 2,6-dimethylaniline provide an opportunity to examine the effect of sterics on the formation of arylamines.

The complex interplay between steric and electronic properties uniquely influenced each catalytic reaction. The electronic effects can be examined by comparing the electronic nature of the substrates and the ligands. Based on the yields, [$PdCl_2$(dppf)] seems to be the best catalyst precursor for alkyl amines and the electron rich aryl bromides. This suggests that the best catalyst for electron rich substrates has the least electron rich ligand. In addition, when electron-poor substrates are used, all of the catalysts examined show poor efficiency. Because one of the first steps in the proposed catalytic mechanism is oxidative addition, it is not surprising that the presence of an electron-withdrawing group is detrimental to the rate of the reaction. In the catalytic reactions with bromotrifluorotoluene, the catalysts with alkyl groups are either similar or superior to dppf and dppr. A similar trend can be observed in the reactions with the less electron rich aniline and 2,6-dimethylaniline.

Sterics effects also play a role in the efficiency of catalysis. When comparing electronically similar amines, the catalysts with smaller bite angles were more efficient with less bulky amines. For example, when comparing cyclohexylamine and hexylamine, [$PdCl_2$(dppf)], the catalyst precursor with the smallest bite angle, gave higher yields when hexylamine, the less hindered of the two amines, was the amine substrate. The same is true when comparing aniline and 2,6-dimethylaniline. The reaction with the less hindered substrate, aniline, catalyzed by [$PdCl_2$(dppf)] gave a higher yield than when the substrate was 2,6-dimethylaniline. This was not unexpected, as the catalysts with larger bite angles have less room on the palladium center for the amine to add. If the amine is bulkier, the addition will be more difficult.

The complex interplay of steric and electronic factors is best observed in the catalysts with alkyl groups on the phosphorus atoms. The *tert*-butyl groups of dtbpf are the most donating and the bulkiest of the alkyl-containing

phosphine ligands studied. Rates with the bulkier amines, cyclohexylamine and 2,6-dimethylaniline, are significantly lower compared to the less bulky amines when [$PdCl_2$(dtbpf)] was used as the catalyst precursor. However, when using bromotrifluorotoluene and aniline as the substrates, the most efficient catalyst precursor is [$PdCl_2$-(dtbpf)]. The steric and electronic nature of the substrates clearly influences which catalyst will be most efficient for the system.

4. Summary

Electrochemical studies of dcpf were carried out and the oxidation is proposed to follow an EC dimerization mechanism. Seven compounds containing dcpf and one compound with dtbpf were synthesized and characterized. The X-ray structure of [$PdCl_2$(dcpf)] was determined, and it showed the pseudo-square planar geometry predicted for d^8 metals. The remaining compounds were characterized by NMR and UV–Vis spectroscopy. Almost all of the compounds showed a downfield shift in the $^{31}P\{^1H\}$ NMR when coordinated to a metal. The oxidative electrochemistry of the dcpf and dtbpf compounds is also reported. Upon coordination, the potential at which oxidation of dcpf and dtbpf occurs is more positive. In addition, the oxidation of compounds containing the 3d metals occurred at less positive potentials than those containing 4d and 5d metals.

The use of [$PdCl_2$(dppf)], [$PdCl_2$(dppr)], [$PdCl_2$(dippf)], [$PdCl_2$(dcpf)] and [$PdCl_2$(dtbpf)] in the formation of aromatic carbon–nitrogen bonds by the Buchwald–Hartwig reaction led to the desired arylamine product. Differences in the electronic and steric properties of the bidentate phosphine ligands on the palladium catalyst affected the efficiency of the catalytic reaction. [$PdCl_2$(dppf)] appears to be the best catalyst precursor unless the substrates are electron poor. The presence of an electron withdrawing group on the aryl bromide led to poor efficiency for all of the catalysts studied. However, catalysts containing alkyl groups rather than aryl groups, as in the case of [$PdCl_2$(dippf)], [$PdCl_2$(dcpf)] and [$PdCl_2$(dtbpf)], were slightly more efficient when coupling electron-poor substrates. When comparing electronically similar amines, catalysts with smaller bite angles were more efficient with less bulky amines. The steric and electronic properties of the substrates play a critical role in determining which catalyst will be most effective for a given coupling.

5. Supplementary material

Crystallographic data (CIF file) for the structural analysis have been deposited with the Cambridge Crystallographic Data Centre, CCDC No. 612566 for [$PdCl_2$(dcpf)] $\cdot$ $2CH_2Cl_2$. Copies of this information may be obtained free of charge from The Director, CCDC, 12 Union Road, Cambridge CB2 1EZ, UK (fax: 44 1223 336033; e-mail: deposit@ccdc.cam.ac.uk or www:http://www.ccdc.cam.ac.uk).

Acknowledgements

L.E.H., A.N.C. and C.N. thank the donors of the Petroleum Research Fund, administered by the American Chemical Society, for partial funding of this research, the Kresge Foundation for the purchase of the JEOL NMR, the Academic Research Committee at Lafayette College for funding EXCEL scholars.

References

[1] S. Shekar, P. Ryberg, J.F. Hartwig, J.S. Mathew, D.G. Blackmond, E.R. Stieter, S.L. Buchwald, J. Am. Chem. Soc. 128 (2006) 3584.
[2] B.C. Hamann, J.F. Hartwig, J. Am. Chem. Soc. 120 (1998) 3694.
[3] B.C. Hamann, J.F. Hartwig, J. Am. Chem. Soc. 120 (1998) 7369.
[4] J.F. Hartwig, S. Richards, D. Baranano, F. Paul, J. Am. Chem. Soc. 118 (1996) 3626.
[5] T. Hayashi, M. Konishi, Y. Kobori, M. Kumada, T. Higuchi, K. Hirotsu, J. Am. Chem. Soc. 106 (1984) 158.
[6] B. Ruhland, A. Bombrun, M.A. Gallop, J. Org. Chem. 62 (1997) 7820.
[7] E. Yoshikawa, K.V. Radhakrishnan, Y. Yamamoto, J. Am. Chem. Soc. 122 (2000) 7280.
[8] P.G. Ciattini, E. Morera, G. Ortar, S.S. Rossi, Tetrahedron 47 (1991) 6449.
[9] T.J. Colacot, H.A. Shea, Org. Lett. 6 (2004) 3731.
[10] T.J. Colacot, Platinum Met. Rev. 45 (2001) 22.
[11] T.J. Colacot, H. Qian, R. Cea-Olivares, S. Hernandez-Ortega, J. Organomet. Chem. 691 (2001) 637–639.
[12] G. Mann, C. Incarvito, A.L. Rheingold, J.F. Hartwig, J. Am. Chem. Soc. 121 (1999) 3224.
[13] N. Kato, N. Miyaura, Tetrahedron 52 (1996) 13347.
[14] M. Kawatsura, J.F. Hartwig, J. Am. Chem. Soc. 121 (1999) 1473.
[15] G. Mann, D. Baranano, J.F. Hartwig, A.L. Rheingold, I.A. Guzei, J. Am. Chem. Soc. 120 (1998) 9205.
[16] S. Rajagopaian, G. Radke, M. Evans, J.M. Tomich, Synth. Commun. 26 (1996) 1431.
[17] M.S. Driver, J.F. Hartwig, J. Am. Chem. Soc. 119 (1997) 8232.
[18] M.S. Driver, J.F. Hartwig, J. Am. Chem. Soc. 118 (1996) 7217.
[19] S. Lee, J.F. Hartwig, J. Org. Chem. 66 (2001) 3402.
[20] M. Kawatsura, J.F. Hartwig, J. Am. Chem. Soc. 121 (1991) 1473.
[21] S. Li, B. Wei, P.M.N. Low, H.K. Lee, T.S.A. Hor, F. Xue, T.C.W. Mak, J. Chem. Soc., Dalton Trans. (1997) 1289.
[22] T.-J. Kim, Y.-H. Kim, H.-S. Kim, S.-C. Shim, Y.-W. Kwak, J.-S. Cha, H.-S. Lee, J.-K. Uhm, S.-I. Byun, Bull. Korean Chem. Soc. 13 (1992) 588.
[23] B. Corain, B. Longato, G. Favero, D. Ajo, G. Pilloni, U. Russo, F.R. Kreissl, Inorg. Chem. Acta 157 (1989) 259.
[24] A.R. Elsagir, F. Gassner, H. Gorls, E. Dinjus, J. Organomet. Chem. 597 (2000) 139.
[25] I.R. Butler, W.R. Cullen, T.J. Kim, S.J. Rettig, J. Trotter, Orgaometallics 4 (1985) 972.
[26] R.J. LeSuer, W.E. Geiger, Angew. Chem., Int. Ed. Engl. 39 (2000) 248.
[27] G.M. Sheldrick, SADABS (2.01), Bruker/Siemens Area Detector Absorption Correction Program, Bruker AXS, Madison, WI, 1998.
[28] P. Van der Sluis, A.L. Spek, Acta Crystallogr. A 46 (1990) 194.

[29] N. Camire, U.T. Mueller-Westerhoff, W.E. Geiger, J. Organomet. Chem. 637–639 (2001) 823, The difference between Fc_* and FcH in CH_2Cl_2 is 0.55 V when the supporting electrolyte contains PF_6^- and 0.62 V when the anion is $B(C_6F_5)_4^-$.
[30] M. Rudolph, D.P. Reddy, S. Feldberg, Anal. Chem. 66 (1994) 589A.
[31] J.H.L. Ong, C. Nataro, J.A. Golen, A.L. Rheingold, Organometallics 22 (2004) 5027.
[32] F.N. Blanco, L.E. Hagopian, W.R. McNamara, J.A. Golen, A.L. Rheingold, C. Nataro, Organometallics 25 (2006) 4292.
[33] S. Lu, V.V. Strelets, M.F. Ryan, W.J. Pietro, A.B.P. Lever, Inorg. Chem. 35 (1996) 1013, From this reference, FcH = 0.66 V vs. NHE.
[34] M.L. Olmstead, R.G. Hamilton, R.S. Nicholson, Anal. Chem. 41 (1969) 260.
[35] A. Lasia, J. Electroanal. Chem. 146 (1983) 413.
[36] W.E. Geiger, in: P.T. Lissinger, W.R. Heineman (Eds.), Laboratory Techniques in Electroanalytical Chemistry, second ed., Marcel Dekker, New York, 1996, p. 683.
[37] C. Nataro, A.N. Campbell, M.A. Ferguson, C.D. Incarvito, A.L. Rheingold, J. Organomet. Chem. 673 (2004) 47.
[38] C.A. Tolman, Chem. Rev. 77 (1977) 313.
[39] G.S. Girolami, T.B. Rauchfuss, R.J. Angelici, in: Synthesis and Technique in Inorganic Chemistry, third ed., University Science Books, Sausalito, CA, 1999, p. 117.
[40] G.L. Miessler, D.A. Tarr, in: Inorganic Chemistry, second ed., Prentice-Hall, Upper Saddle River, NJ, 1999, p. 315.
[41] (a) K.-S. Gan, T.S.A. Hor, in: A. Togni, T. Hayashi (Eds.), Ferrocenes from Homogeneous Catalysis to Material Science, VCH, New York, 1995, p. 3;
(b) G. Bandoli, A. Dolmella, Coord. Chem. Rev. 209 (2000) 161.
[42] G.M. de Lima, C.A.L. Filgueiras, M.T.S. Giotto, Y.P. Mascarenhas, Transition Met. Chem. 20 (1995) 380.
[43] R.J. Angelici, Acc. Chem. Res. 28 (1995) 51.
[44] Z. Fang, P.M.N. Low, S. Ng, T.S.A. Hor, J. Organomet. Chem. 483 (1994) 17.
[45] A.R. O'Connor, C. Nataro, Organometallics 23 (2004) 615.
[46] C. Hansch, A. Leo, R.W. Taft, Chem. Rev. 91 (1991) 165.
[47] S.L. Martinak, L.A. Sites, S.J. Kolb, K.M. Bocage, W.R. McNamara, A.L. Rheingold, J.A. Golen, C. Nataro, J. Organomet. Chem. 691 (2006) 3627.
[48] C. Bianchini, A. Meli, W. Oberhauser, S. Parisel, E. Passaglia, F. Ciardelli, O.V. Gusev, A.M. Kal'sin, N.V. Vologdin, Organometallics 24 (2005) 1018.